 https://doi.org/10.3311/PPch.13873

Periodica Polytechnica Chemical Engineering, 63(3), pp. 378–387, 2019

Photocatalytically Active Amorphous and Crystalline TiO_2 Prepared by Atomic Layer Deposition

Orsolya Kéri[1*], Lenke Kócs[2], Zoltán Hórvölgyi[2], Zsófia Baji[3], Krisztina László[2], Viktor Takáts[4], Zoltán Erdélyi[5], Imre Miklós Szilágyi[1]

[1] Department of Inorganic and Analytical Chemistry, Faculty of Chemical Technology and Biotechnology, Budapest University of Technology and Economics, H-1111 Budapest, Szt. Gellért tér 4., Hungary
[2] Department of Physical Chemistry and Materials Science, Faculty of Chemical Technology and Biotechnology, Budapest University of Technology and Economics, H-1111 Budapest, Budafoki út 6-8., Hungary
[3] Hungarian Academy of Sciences, Centre for Energy Research, Institute for Technical Physics, H–1121 Budapest, Konkoly–Thege út 29–33., Hungary
[4] Hungarian Academy of Sciences, Institute for Nuclear Research (Atomki), H–4026 Debrecen, Bem tér 18/c., Hungary
[5] Department of Solid State Physics, Faculty of Sciences and Technology, University of Debrecen, H–4026 Debrecen, Bem tér 18/b., Hungary
* Corresponding author, e-mail: keri.orsolya@mail.bme.hu

Received: 12 February 2019, Accepted: 03 March 2019, Published online: 26 March 2019

Abstract

In this work, the photocatalytic properties of amorphous and crystalline TiO_2 deposited on oxide and polymer nanoparticles by atomic layer deposition (ALD) were studied. Beside TiO_2, as reference, both ALD grown amorphous Al_2O_3 and crystalline ZnO layers were also examined. When choosing the carrier, the priority was that it had no effect on the photocatalytic activity of TiO_2; therefore the oxide layers were deposited on SiO_2 and poly(methyl-methacrylate) (PMMA) nanoparticles. The amorphous SiO_2 particles were synthetized by the Stöber method, while the PMMA particles were prepared by emulsion polymerization. Both the bare and core/shell composite nanoparticles were investigated by SEM-EDX, TEM, FT-IR, and XRD. Finally, the photocatalytic activity of PMMA, SiO_2 and the core/shell nanoparticles was measured by the decomposition of methylene orange, monitored by UV-Vis spectroscopy. Based on the results, the SiO_2 was uniformly coated with the deposited oxide films, while in the case of the PMMA a contiguous web-like polymer/TiO_2 matrix was formed. During the photocatalytic reactions, the amorphous Al_2O_3 was not active, while the crystalline ZnO and TiO_2 showed good photocatalytic activity. The amorphous TiO_2 deposited by ALD on the SiO_2 and PMMA nanoparticles had smaller, but a clearly detectable photocatalytic effect on the photodegradation of methylene orange.

Keywords

titanium-dioxide, amorphous, crystalline, atomic layer deposition, photocatalysis

1 Introduction

It has long been an important issue how the energy of the sunlight can be effectively converted into chemical energy [1], and in recent years the interest in semiconductor oxide photocatalysts such as WO_3, ZnO, and TiO_2 has grown exponentially [2]. These photocatalysts are widely used in water purification [3, 4], decomposition of organic contaminants [5–7] or in the preparation of self-cleaning surfaces [8, 9]. TiO_2 is the most widespread out of the semiconductor oxides in these fields, due to its low cost, good physical and chemical stability and being environmentally friendly.

TiO_2 has three crystalline forms: anatase, rutile, and brookite. Since the 1960s all forms of crystalline TiO_2 have been thoroughly investigated in photocatalytic reactions, e.g. in the splitting of water and in many other reactions [10, 11]. It was revealed that generally anatase TiO_2 was more active than rutile [12], while brookite was not investigated thoroughly due to the difficulties in obtaining it as a pure phase. In some cases it was proved that brookite could have even higher photocatalytic activity than anatase [13]; however, its application is hindered, thanks to the complicated and relatively expensive preparations methods [14]. It has also been found that the photocatalytic activity of crystalline TiO_2 can be increased and shifted to visible light by doping it with heteroatoms (e.g. C, N,

Cite this article as: Kéri, O., Kócs, L., Hórvölgyi, Z., Baji, Zs., László, K., Takáts, V., Erdélyi, Z., Szilágyi, I. M. "Photocatalytically Active Amorphous and Crystalline TiO2 Prepared by Atomic Layer Deposition", Periodica Polytechnica Chemical Engineering, 63(3), pp. 378–387, 2019. https://doi.org/10.3311/PPch.13873

S) [15, 16] and other metal atoms [17, 18] or by using it in composites with different semiconductor oxides [19–21].

Amorphous TiO_2 in itself is considered not to have any photocatalytic property, because the defects in the crystal structure can serve as recombination centers [22]. Nevertheless, it was observed that if magnetron sputtered amorphous TiO_2 was coupled with other semiconductor oxides, the amorphous material alone was inactive, but the composites showed photo-reactivity and the response could be expanded to the visible region [23]. Recently it was also discovered that amorphous TiO_2 grown by atomic layer deposition (ALD) on lotus leaves could show some photocatalytic activity [24]. ALD is a self-limiting, sequential thin film deposition method; owing to the alternating surface-controlled reactions in the ALD reactor the growth of thin films from the gas phase is possible within nanometer range precision [25–27]. This technique allows the coating of flat surfaces, nanoparticles and even nanofibers [28, 29] with amorphous or crystalline oxide layers depending on the deposition temperature and among other applications these core/shell nanocomposites can be used as photocatalysts.

Hence, we investigated ALD grown amorphous and crystalline TiO_2, deposited onto SiO_2 and PMMA nanoparticles and compared the photocatalytic properties. SiO_2 and PMMA were chosen as carriers, because they did not affect the course of the photocatalytic reactions, and hence the efficiency was only dependent on the TiO_2 shell. First, the carrier particles were prepared, i.e. the SiO_2 by the Stöber method, while the PMMA nanoparticles by emulsion polymerization. After that, the TiO_2 was deposited onto them, and as a reference, amorphous Al_2O_3 and crystalline ZnO layers were also grown on the SiO_2 nanoparticles by ALD. All samples were investigated by SEM-EDX, TEM, FT-IR, and XRD. Finally, the photocatalytic activities were measured by the decomposition of methylene orange, monitored by UV-Vis spectroscopy.

2 Experimental

The SiO_2 nanoparticles were prepared by the Stöber method [30,31] from tetraethyl orthosilicate (TEOS). 8 cm^3 TEOS was added to a mixture of 200 cm^3 ethanol and 12 cm^3 25 % ammonium hydroxide. The solution was stirred for 24 h at room temperature, during which in various hydrolysis and polycondensation steps SiO_2 nanoparticles were formed.

The poly(methyl methacrylate) (PMMA) nanoparticles were prepared by emulsion polymerization [32] from methyl methacrylate monomer, using potassium peroxodisulfate as the initiator and sodium lauryl sulfate as the emulsifier. From the methyl methacrylate 25.81 g was mixed with 180 g distilled water, 0.18 g sodium lauryl sulfate, and 0.18 g potassium peroxodisulfate. The reaction mixture was continuously stirred at 80 °C under nitrogen atmosphere. The completion of the reaction was indicated by the disappearance of the characteristic odor of the monomer. After cooling the mixture to room temperature the polymer nanoparticles were precipitated with the addition of 400 cm^3 1 M HCl solution. The SiO_2 and PMMA particles were separated from the liquid phases by centrifuging (3000 rpm, 10 min), then those were washed 3 times with distilled water and dried in air at room temperature.

The deposition of ALD thin films on the nanoparticles was done in a Picosun SUNALE R-100 reactor. The overall pressure in the reactor chamber was around 10 mbar during all the reactions. The TiO_2 films were prepared using titanium tetraisopropoxide (TTIP) and H_2O as precursors. Before coating the nanoparticles, it had to be determined from what deposition temperature the produced TiO_2 layer was crystalline. For this several depositions were done onto Si wafers at different temperatures from 80 °C to 300 °C (80 °C, 160 °C, 200 °C, 250 °C, 300 °C). In this case, the precursor pulse time was 0.1 s for both TTIP and H_2O with a 3 s purge after the TTIP and a 4 s purge after the H_2O pulses. The TiO_2 was deposited in 1000 cycles. After this, the preparation of the TiO_2 layers was done at 80 °C and 300 °C on the SiO_2 and only at 80 °C on the PMMA particles. Beside the TiO_2 coatings, as reference, Al_2O_3 and ZnO were also grown at 80 °C and 250 °C. The Al_2O_3 films were synthetized from trimethylaluminium (TMA) and H_2O as precursors, while ZnO from diethylzinc (DEZ) and H_2O. In the preparation of the nanocomposites, the TTIP, DEZ, TMA and H_2O pulse times were all 0.5 s. The purge times were uniformly 15 s after the precursors. The TiO_2 was deposited in 250, while the Al_2O_3 and ZnO in 100 cycles.

The composition of the samples was studied with energy dispersive X-ray (EDX) analysis in a JEOL JSM-5500LV scanning electron microscope. The measurements were done at 20 kV voltage. Before the measurement, the nanocomposites were coated with a thin Au/Pd layer in a sputter coater.

X-ray photoelectron spectra (XPS) were taken on a PHOIBOS HSA3500 100 R6 device. Before the measurement the powders were pressed to obtain pellets, the surface of the pellets were argon sputter cleaned.

The XRD patterns were recorded with a PANalytical X'pert Pro MPD X-ray diffractometer using Cu K_α irradiation.

The FTIR spectra of the composites were measured by a Biorad Excalibur Series FTS 3000 FTIR spectrophotometer between 400 and 4000 cm^{-1} in KBr pellets.

TEM images were taken by an FEI Morgagni 268 TEM microscope.

Nitrogen adsorption/desorption isotherms were measured at -196 °C with a Nova2000e (Quantachrome) computer-controlled apparatus. The apparent surface area (SBET) was calculated using the Brunauer–Emmett–Teller (BET) model [33].

The photocatalytic properties of the samples were studied by decomposing methyl orange (MO) dye. 1 mg of the nanocomposites was put into 3 cm^3 aqueous 0.04 mM MO solution, kept in the dark for 1 h for adsorbing the dye, then illuminated by two parallel UV backlights (Osram blacklight UV-A, 18 W) that were placed 5 cm from the samples on either side. The measured wavelength of the lamp is between 350-390 nm (maximum intensity at 375 nm) (Fig. 1), and the estimated power at the samples is 0.5 W. The UV-Vis spectra of the MO solutions were measured every 30 minutes during the photocatalytic reactions by a Jasco V-550 UV-VIS spectrophotometer. The relative absorbance values, which were plotted versus time, were determined at the 464 nm absorption peak. As a reference the samples were compared to P25 TiO_2 (Aeroxide) measured under the same conditions.

3 Result and Discussion

Before the preparation of the composites, the ALD deposition temperature was determined in order to grow both amorphous and crystalline TiO_2. The layers were synthetized onto Si wafers and the crystallinity was checked by XRD. On Fig. 2 it is visible that till 200 °C only the peaks referring to crystalline Si are visible (33° and 62°, ICDD 00-040-0932), therefore the TiO_2 layer is amorphous, but from 250 °C, the pattern of anatase TiO_2 (25° and 48°, ICDD 01-083-2243) appears on the diffractogram. Based on these findings, later the deposition of TiO_2 onto the nanoparticle substrates was done at 80 °C and 300 °C in order to be able to compare the properties of the amorphous layers with that of the crystalline ones. The reference Al_2O_3 and ZnO layers were grown at 80 °C and 250 °C.

The preparation of SiO_2 nanoparticles by sol-gel method and the synthesis of the PMMA particles by emulsion polymerization were successful. It can be seen in the TEM images (Fig. 3a-b and Fig. 4a-b) that in both cases the particles were spherical; the SiO_2 nanoparticles had a diameter of 100-150 nm (Fig. 3 a-b), while the size of the PMMA particles was 50-100 nm (Fig. 4 a-b).

After the deposition, the composites were investigated with TEM again (Fig. 3 and Fig. 4). In the case of the SiO_2 substrate (Fig. 3 c-h), it was visible that core/shell structured nanoparticles were successfully prepared, the thickness of the deposited oxide layers was about 10-20 nm in all samples. This showed that the growth-per-cycle (GPC) [34] value for these oxides vary greatly, i.e. achieving the same

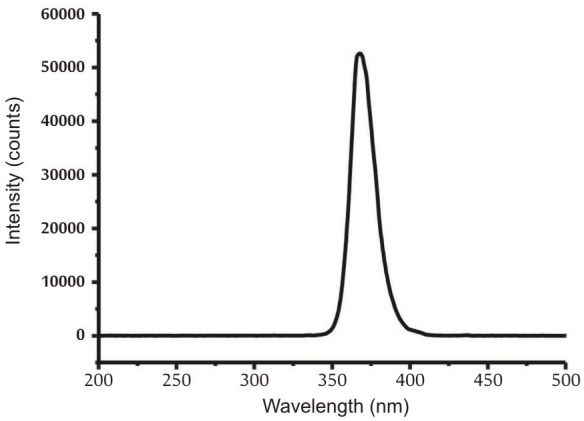

Fig. 1 Emittance of the UV blacklight source

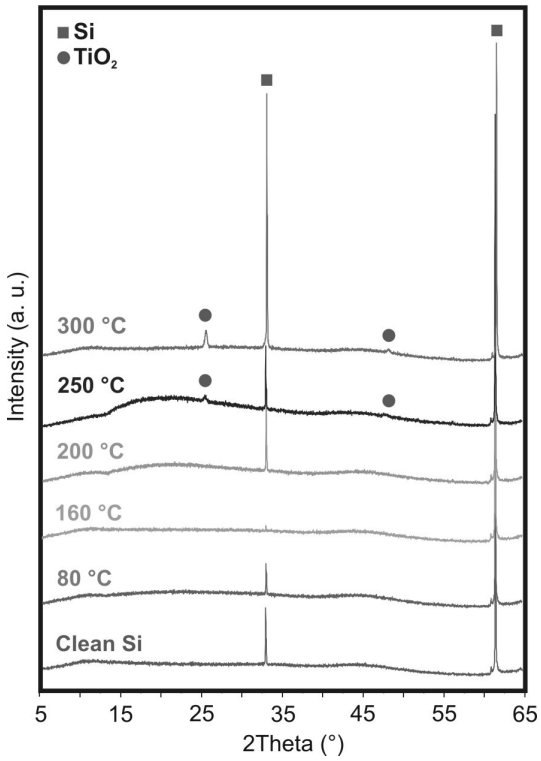

Fig. 2 XRD results of TiO_2 deposited at different temperatures onto Si wafers

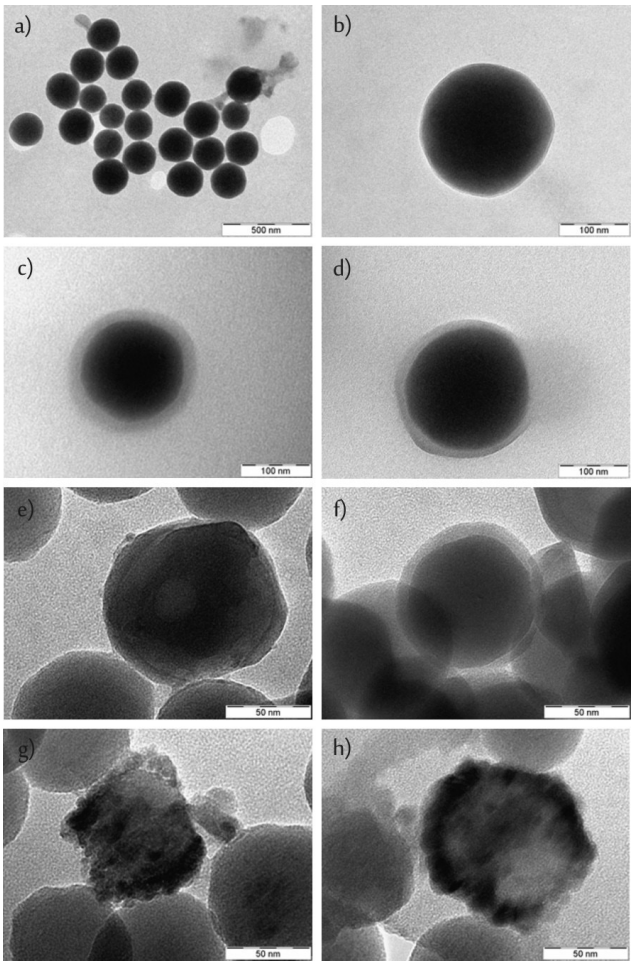

Fig. 3 TEM images of a-b) the SiO_2 nanoparticles and the SiO_2/oxide nanocomposites; c) SiO_2/TiO_2 (80 °C), d) SiO_2/TiO_2 (300 °C), e) SiO_2/Al_2O_3 (80 °C), f) SiO_2/Al_2O_3 (250 °C), g) SiO_2/ZnO (80 °C), h) SiO_2/ZnO (250 °C)

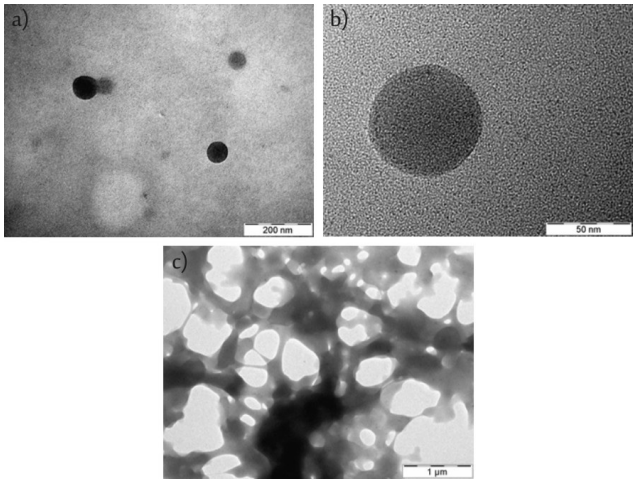

Fig. 4 TEM images of a-b) the PMMA nanoparticles and c) the PMMA/TiO_2 nanocomposites

Table 1 Composition of the core/shell nanoparticles measured by EDX

Element	C	Si	O	Ti	Al	Zn
	$^m/_m$ %					
PMMA/TiO_2 80 °C	71.1	-	26.2	2.7	-	-
SiO_2/TiO_2 80 °C	-	51.3	40.4	8.3	-	-
SiO_2/TiO_2 300 °C	-	43.9	46.1	10.0	-	-
SiO_2/Al_2O_3 80 °C	-	24.4	63.1	-	12.6	-
SiO_2/Al_2O_3 250 °C	-	25.6	60.2	-	14.2	-
SiO_2/ZnO 80 °C	-	24.4	24.1	-	-	51.5
SiO_2/ZnO 250 °C	-	24.5	32.2	-	-	43.4

thickness for the TiO_2 layer as the Al_2O_3 and ZnO required 2.5 times as many cycles. The TiO_2 and Al_2O_3 formed uniform and even coatings, while the ZnO layer consisted of smaller, aggregated particles. It was visible in the TEM images that the PMMA particles (Fig. 4 c) softened during the preparation of the composites, and a contiguous matrix was formed from the polymer and the oxide, which could have been caused by the exoterm nature of the ALD reactions. Therefore not core/shell PMMA/TiO_2 particles, but a PMMA/TiO_2 web-like nanostructure was obtained.

The EDX results (Table 1) also proved that the ALD depositions were successful; Ti, Al, and Zn could be found in the samples. The amount of Al_2O_3 grown at different temperatures was the same, but at 250 °C smaller amount of ZnO was deposited than at 80 °C. This can be explained by that at 250 °C the upper limit of the ZnO ALD window was reached [35]. The SiO_2/TiO_2 nanocomposite sample prepared at higher temperature contained more TiO_2 than the 80 °C composite, while when the PMMA was used as carrier, the amount of deposited TiO_2 was the lowest. This can be explained by the presence of less functional groups on the surface of PMMA, than on the SiO_2.

From the XRD patterns (Fig. 5) it can be seen that after the deposition the TiO_2 is amorphous when deposited at 80 °C and crystalline at 300 °C, but the Al_2O_3 is amorphous and the ZnO is crystalline (zincite, ICDD 00-036-1451) at both temperatures (80 °C and 250 °C). Based on the Scherrer-equation the crystallite size of the ZnO was about 20 nm, which was in accordance with the ZnO particle size on the TEM images. This was determined for the crystalline TiO_2 layer as well, but the calculated value of about 20 nm is rather an estimate for the thickness of the

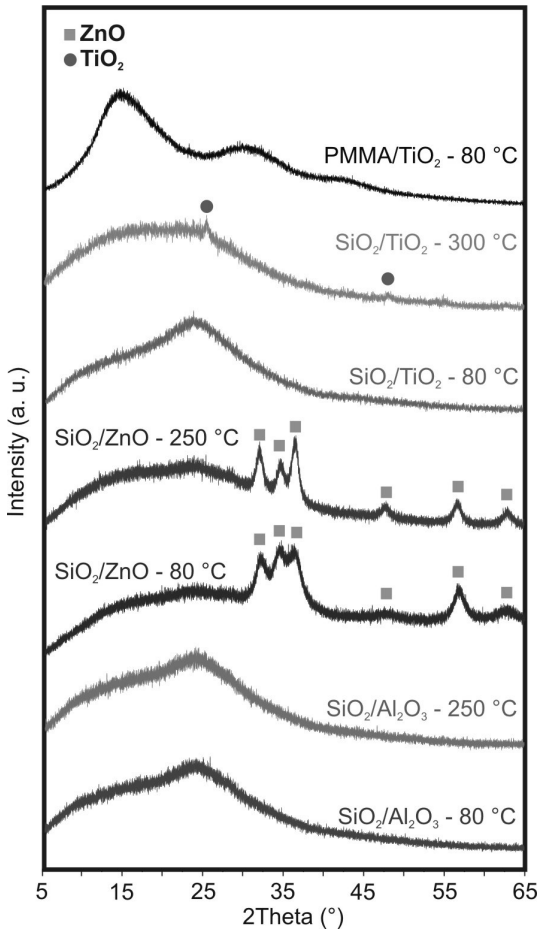

Fig. 5 XRD measurement of the core/shell nanocomposites

TiO_2 film, since it was a continuous layer, and not made up by individual particles like the ZnO shell. In the case of amorphous TiO_2 during the TEM measurements the electron diffraction was investigated as well to confirm that the samples did not contain nanocrystalline domains. There were no observable electron diffraction patterns, thus these samples were completely amorphous.

In the FTIR spectra (Fig. 6) of the samples containing SiO_2, the peaks at 3410 cm^{-1} and 1634 cm^{-1} correspond to the vibrations of the surface O-H groups and the absorbed water. The 949 cm^{-1} is the stretching vibration of the Si-OH bond and the peaks at 1099 cm^{-1}, 799 cm^{-1}, 468 cm^{-1} are the stretching, bending and out of plane rocking of Si-O and Si-O-Si bonds [36, 37]. In the spectra of the PMMA, the 3441 cm^{-1} peak refers again to the adsorbed water. The peaks at 2997 cm^{-1} and 2951 cm^{-1} can be assigned to the stretching, the 1449 cm^{-1} peak to the bending vibrations of C-H bonds. The 1730 cm^{-1} peak can indicate the presence of the acrylate carboxyl group, while the 750 cm^{-1} one is referring to the α-methyl groups. The 1242 cm^{-1} and 1150 cm^{-1} peaks can be attributed to the C-O-C stretching vibrations. The bands

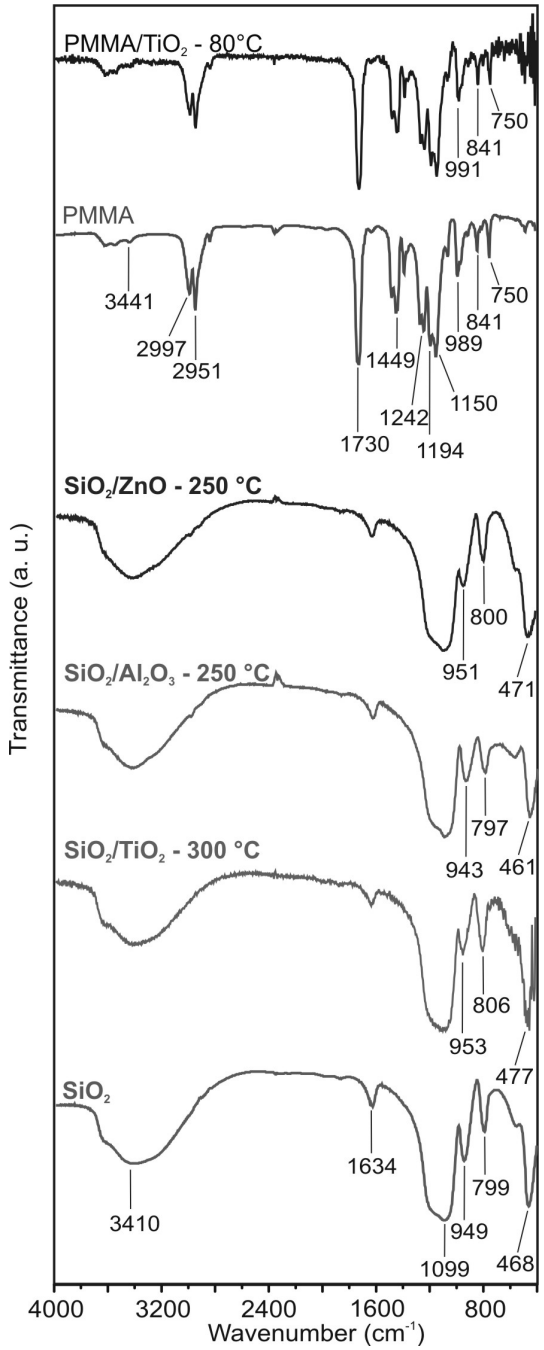

Fig. 6 FTIR measurement of the pure nanoparticles and core/shell nanocomposites

at 989 cm^{-1} and 841 cm^{-1} are characteristic PMMA absorption vibrations [38, 39]. The TiO_2, ZnO and Al_2O_3 lattice vibrations are expected below 1000 cm^{-1}. On the spectra, the slight shift in the position of the peaks between 1000-400 cm^{-1} and the changes in the ratio of intensity can refer to the presence of the ALD deposited oxide.

For the samples containing TiO_2 some further measurements were carried out. The specific surface area of the samples was determined based on nitrogen adsorption/

desorption isotherms (Table 2). After the deposition, for the PMMA/TiO_2 composite the surface area decreased slightly, which can be attributed to the change in the shape of the PMMA substrate. In the case of the SiO_2/TiO_2 composites, at 80 °C the surface area did not differ much from the pure SiO_2 substrate, while after the 300 °C deposition there was a considerable decrease. This was possibly due to the sintering of the SiO_2/TiO_2 particles at the higher deposition temperature.

Also the chemical composition of the ALD TiO_2 layer was further investigate by XPS measurements (Fig. 7), for this the Ti 2p peaks were decomposed by a standard non-linear least-squares fitting method. Based on the results, next to TiO_2, Ti was present in the form of Ti_2O_3 suboxide phase as well on the surface of the sample. The formation of this phase on ALD layers and other TiO_2 samples was already described in the literature, and in some cases it was found to be thermodynamically favored [40, 41].

The result of the photocatalytic measurements (Fig. 8) of the composites containing Al_2O_3 and ZnO have met the expectations. The amorphous Al_2O_3 layer had no photocatalytic property (Fig. 8a), i. e. the SiO_2/Al_2O_3 prepared both at 80°C and 250 °C had the same effect as the substrate SiO_2, while the crystalline ZnO layer had good photocatalytic properties (Fig. 6b). The SiO_2/ZnO composite that was synthetized at 80 °C had a higher efficiency, because it contained more crystalline ZnO. The SiO_2/crystalline TiO_2 sample (Fig. 8c) had similar activity as the SiO_2/ZnO samples. Interestingly this sample had a very low specific surface area, but a good photocatalytic efficiency. The SiO_2/amorphous TiO_2 core/shell nanoparticles had low activity; however, it clearly had higher decomposition rate than the SiO_2 substrate, pointing to a small, but observable photocatalytic effect of amorphous TiO_2. In the case of PMMA/amorphous TiO_2 nanocomposite (Fig. 8d), the small, but detectable photocatalytic property of amorphous TiO_2 was even more visible. This was a surprising effect, since previously it was only observed when charge separation was possible between the substrate and the coating [24, 42]. The photocatalytic properties of the two samples that had the highest efficiency (SiO_2/ZnO - 80 °C, SiO_2/TiO_2 - 300 °C) were compared to P25 TiO_2 (Fig. 9a). Both samples that were synthetized by ALD had a higher photocatalytic activity than the P25 TiO_2 measured under the same conditions. The apparent reaction rate constants,

Table 2 Specific surface area of the pure nanoparticles and the samples containing TiO_2

Sample	s(BET)
	m^2/g
PMMA	56
PMMA/TiO_2 80 °C	50
SiO_2	14
SiO_2/TiO_2 80 °C	17
SiO_2/TiO_2 300 °C	1

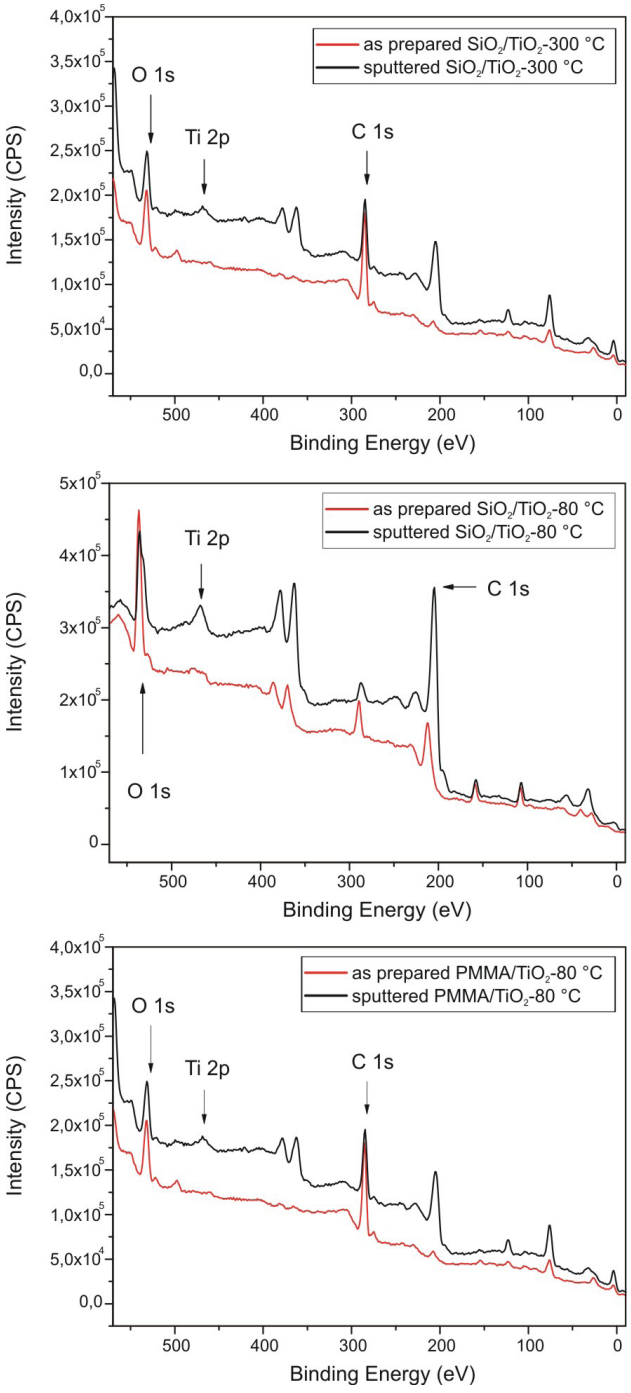

Fig. 7 XPS results of the samples containing TiO_2

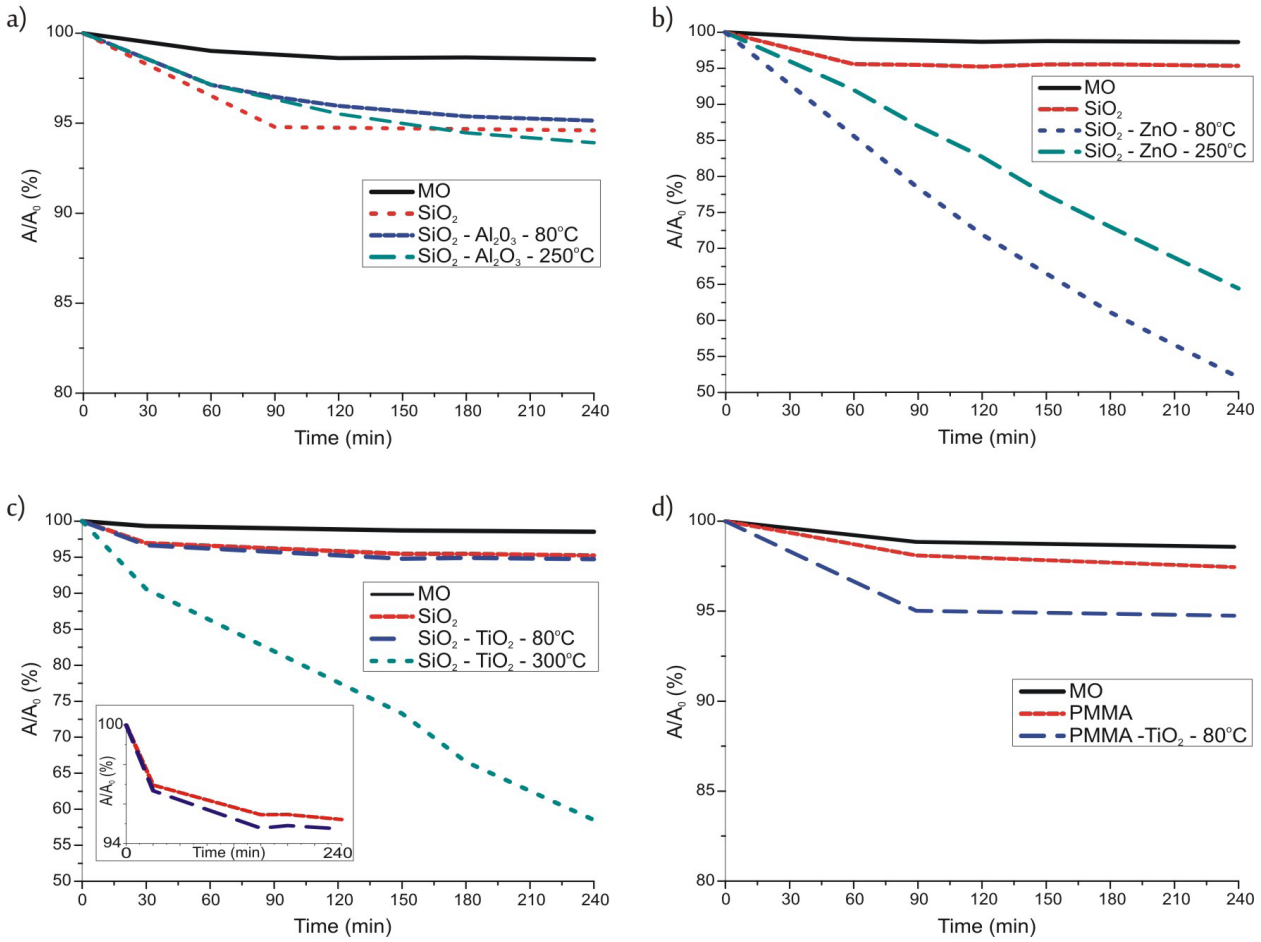

Fig. 8 Photocatalytic efficiency of the prepared nanocomposites

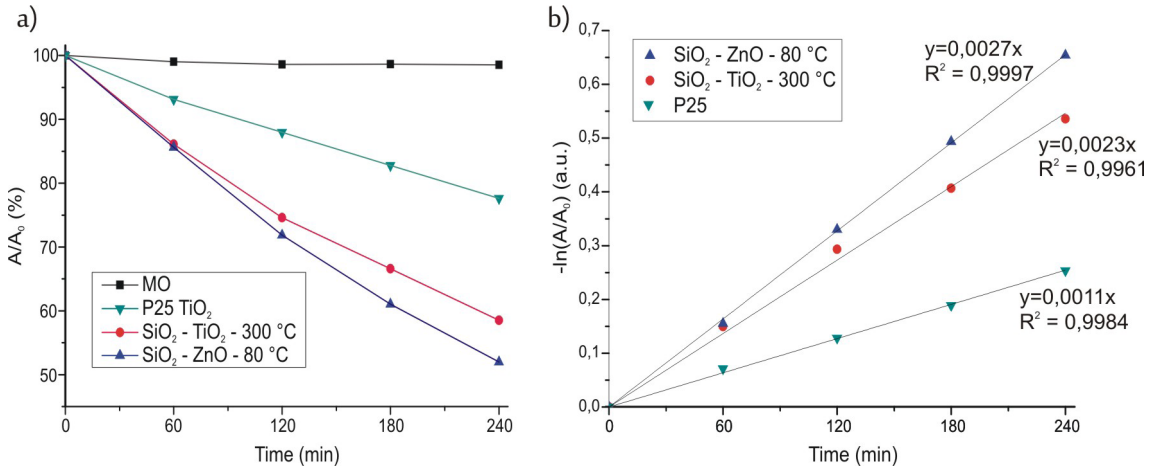

Fig. 9 a) Photocatalytic efficiency of the SiO_2/ZnO – 80 °C and SiO_2/TiO_2 – 300 °C compared to P25 TiO_2; b) kinetics of the photocatalytic reactions

which were indicated by the slope of the fitted lines on Fig. 9b, were determined assuming pseudo first order reaction kinetics. The reaction rate constants in the case of the SiO_2/ZnO - 80 °C, SiO_2/TiO_2 - 300 °C samples were more than two times higher than that of the P25 TiO_2.

4 Conclusion

The photocatalytic properties of amorphous and crystalline TiO_2 thin films deposited by atomic layer deposition (ALD) were studied. With ALD the amorphous and crystalline layers could be prepared with the same morphology and their

photocatalytic properties could be investigated in comparison with each other. As carrier SiO_2 and PMMA nanoparticles were chosen, because those did not interact with the TiO_2 during photocatalytic reactions. About 20 nm thick TiO_2 layers were grown at different deposition temperatures (80 °C, 300 °C); and as reference, the SiO_2 nanoparticles were covered with amorphous Al_2O_3 and crystalline ZnO as well at 80 °C and 250 °C. The TEM images revealed that the SiO_2 nanoparticles were uniformly coated with the deposited oxide films and the PMMA formed a web-like structure with the TiO_2. During the photocatalytic reactions, the amorphous Al_2O_3 was not active, while the crystalline ZnO and TiO_2 showed good photocatalytic activity. The amorphous TiO_2 deposited by ALD on the SiO_2 and PMMA had smaller, but clearly detectable photocatalytic effect. This was an unexpected and previously not described phenomenon. For this behavior we assume three possible reasons: (1) the coating interacts with the substrate during the photocatalytic reactions, (2) the samples contain nanocrystalline domains or (3) there is a small amount of dopant C atoms left over from the ALD precursor (TTIP) in the TiO_2 layers. In our case, between the TiO_2 and chosen carriers (amorphous SiO_2 and PMMA) there is no possibility for charge separation, and it was also confirmed by XRD and electron diffraction measurements that the samples were completely amorphous. A detailed computational chemistry investigation could provide useful answers to these questions; however, that is beyond the scope of the present work. According to the results, the synthesis of amorphous TiO_2 layers does not require high deposition temperature, so the films might be grown by ALD on heat sensitive, highly structured substrates and used for e.g. in the preparation of self-cleaning surfaces.

Acknowledgements

I. M. Szilágyi thanks for a János Bolyai Research Fellowship of the Hungarian Academy of Sciences and an ÚNKP-18-4-IV-BME-238 grant supported by the ÚNKP-17-4-IV New National Excellence Program of the Ministry of Human Capacities, Hungary. The research was financed by the Higher Education Institutional Excellence Programme of the Ministry of Human Capacities in Hungary, within the framework of the Energetics thematic programme of the University of Debrecen. An OTKA PD-109129 grant and a K 124212 grant are acknowledged. The research within project No. VEKOP-2.3.2-16-2017-00013 was supported by the European Union and the State of Hungary, co-financed by the European Regional Development Fund. József Hári and Levente Kárpáti (Budapest University of Technology and Economics, Department of Physical Chemistry and Materials Science) are acknowledged for their support in PMMA nanoparticle preparation.

References

[1] Grätzel, M. "Photoelectrochemical Cells", Nature, 414(6861), pp. 338–344, 2001. https://doi.org/10.1038/35104607

[2] Hoffmann, M. R., Martin, S. T., Choi, W., Bahnemann, D. W. "Environmental Applications of Semiconductor Photocatalysis", Chemical Reviews, 95(1), pp. 69–96, 1995. https://doi.org/10.1021/cr00033a004

[3] Baruah, S., Najam, M., Joydeep, K. "Perspectives and Applications of Nanotechnology in Water Treatment", Environonmental Chemistry Letters, 14(1), pp. 1–14, 2016. https://doi.org/10.1007/s10311-015-0542-2

[4] Sreeja, S., Shetty, K. V. "Photocatalytic Water Disinfection under Solar Irradiation by Ag@TiO_2 Core-Shell Structured Nanoparticles", Solar Energy, 157(15), pp. 236–243, 2017. https://doi.org/10.1016/j.solener.2017.07.057

[5] Fujishima, A., Zhang, X., Tryk, D. "TiO_2 Photocatalysis and Related Surface Phenomena", Surface Science Reports, 63(12), pp. 515–582, 2008. https://doi.org/10.1016/j.surfrep.2008.10.001

[6] Jallouli, N., Pastrana-martínez, L. M., Ribeiro, A. R., Moreira, N. F. F., Faria, J. L., Hentati, O., Silva, A. M. T., Ksibi, M. "Heterogeneous Photocatalytic Degradation of Ibuprofen in Ultrapure Water, Municipal and Pharmaceutical Industry Wastewaters Using a TiO_2/UV-LED System", Chemical Engineering Journal, 334(15), pp. 976–984, 2017. https://doi.org/10.1016/j.cej.2017.10.045

[7] Réti, B., Kiss, G. I., Gyulavári, T., Baan, K., Magyari, K., Hernadi, K. "Carbon Sphere Templates for TiO_2 Hollow Structures: Preparation, Characterization and Photocatalytic Activity", Catalysis Today, 284(15), pp. 160–168, 2017. https://doi.org/10.1016/j.cattod.2016.11.038

[8] Krishna, M. G., Vinjanampati, M., Purkayastha, D. D. "Metal Oxide Thin Films and Nanostructures for Self-Cleaning Applications : Current Status and Future Prospects", The European Physical Journal, Applied Physics, 62(3), pp. 1–12, 2013. https://doi.org/10.1051/epjap/2013130048

[9] Gholami, A., Alemrajabi, A. A.; Saboonchi, A. "Experimental Study of Self-Cleaning Property of Titanium Dioxide and Nanospray Coatings in Solar Applications", Solar Energy, 157(15), pp. 559–565, 2017. https://doi.org/10.1016/j.solener.2017.08.075

[10] Schneider, J., Matsuoka, M., Takeuchi, M., Zhang, J., Horiuchi, Y., Anpo, M., Bahnemann, D. W. "Understanding TiO_2 Photocatalysis : Mechanisms and Materials", Chemical Reviews, 114(19), pp. 9919–9986, 2014. https://doi.org/10.1021/cr5001892

[11] Hashimoto, K., Irie, H., Fujishima, A. "TiO_2 Photocatalysis: A Historical Overview and Future Prospects", Japanese Journal of Applied Physics, 44(12), pp. 8269–8285, 2005. https://doi.org/10.1143/JJAP.44.8269

[12] Luttrell, T., Halpegamage, S., Tao, J., Kramer, A., Sutter, E., Batzill, M. "Why Is Anatase a Better Photocatalyst than Rutile? - Model Studies on Epitaxial TiO_2 Films", Scientific Reports, 4(4034), pp. 1–8, 2014.
https://doi.org/10.1038/srep04043

[13] Kandiel, T. A., Robben, L., Alkaim, A., Bahnemann, D. "Brookite versus Anatase TiO_2 Photocatalysts : Phase Transformations and Photocatalytic Activities", Photochemical and Photobiological Sciences, 12(4), pp. 602–609, 2013.
https://doi.org/10.1039/c2pp25217a

[14] Di Paola, A., Bellardita, M., Palmisano, L. "Brookite, the Least Known TiO_2 Photocatalyst", Catalysts, 3(1), pp. 36–73, 2013.
https://doi.org/10.3390/catal3010036

[15] Khang, N. C., Minh, N. Van, Yang, I. "Synthesis and Characterization of the N-Doped TiO_2 Photocatalyst for the Photodegradation of Methylene Blue and Phenol", Journal of Nanoscience and Nanotechnology, 11(7), pp. 1–5, 2011.
https://doi.org/10.1166/jnn.2011.4508

[16] Sharotri, N., Sud, D. "Visible Light Responsive Mn-S-Co-Doped TiO_2 Photocatalyst- Synthesis, Characterization and Mechanistic Aspect of Photocatalytic Degradation", Separation and Purification Technology, 183, pp. 382–391, 2017.
https://doi.org/10.1016/j.seppur.2017.03.053

[17] Reyes, M. H., Luis, J., Mar, G. "Fe Doped TiO_2 Photocatalyst for the Removal of As(III) under Visible Radiation and Its Potential Application on the Treatment of As-Contaminated Groundwater", Materials Research Bulletin, 73, pp. 145–152, 2016.
https://doi.org/10.1016/j.materresbull.2015.08.034

[18] Bashiri, R., Mohamed, N. M., Kait, C. F., Sufian, S., Khatani, M., Hanaei, H. "Effect of Preparation Parameters on Optical Properties of Cu and Ni Doped TiO_2 Photocatalyst", Procedia Engineering, 148, pp. 151–157, 2016.
https://doi.org/10.1016/j.proeng.2016.06.506

[19] Szilágyi, I. M., Santala, E., Heikkilä, M., Pore, V., Kemell, M., Nikitin, T., Teucher, G., Firkala, T., Khriachtchev, L., Räsänen, M., Ritala, M., Leskelä, M. "Photocatalytic Properties of WO_3/TiO_2 Core/Shell Nanofibers Prepared by Electrospinning and Atomic Layer Deposition", Chemical Vapor Deposition, 19(4–6), pp. 149–155, 2013.
https://doi.org/10.1002/cvde.201207037

[20] Dong, W., Sun, Y., Ma, Q., Zhu, L., Hua, W., Lu, X., Zhuang, G., Zhang, S., Guo, Z., Zhao, D. "Excellent Photocatalytic Degradation Activities of Ordered Mesoporous Anatase TiO_2-SiO_2 Nanocomposites to Various Organic Contaminants", Journal of Hazardous Materials, 229–230, pp. 307–320, 2012.
https://doi.org/10.1016/j.jhazmat.2012.06.002

[21] Bellardita, M., Addamo, M., Di Paola, A., Marcì, G., Palmisano, L., Cassar, L., Borsa, M. "Photocatalytic Activity of TiO_2/SiO_2 Systems", Journal of Hazardous Materials, 174(1–3), pp. 707–713, 2010.
https://doi.org/10.1016/j.jhazmat.2009.09.108

[22] Kaur, K., Singh, C. V. "Amorphous TiO_2 as a Photocatalyst for Hydrogen Production: A DFT Study of Structural and Electronic Properties", Energy Procedia, 29, pp. 291–299, 2012.
https://doi.org/10.1016/j.egypro.2012.09.035

[23] Huang, J., Liu, Y., Lu, L., Li, L. "The Photocatalytic Properties of Amorphous TiO_2 Composite Films Deposited by Magnetron Sputtering", Research on Chemical Intermediates, 38(2), pp. 487–498, 2011.
https://doi.org/10.1007/s11164-011-0365-0

[24] Szilágyi, I. M., Teucher, G., Härkönen, E., Färm, E., Hatanpää, T., Nikitin, T., Khriachtchev, L., Räsänen, M., Ritala, M., Leskelä, M. "Programming Nanostructured Soft Biological Surfaces by Atomic Layer Deposition", Nanotechnology, 24(24), ID. 245701, 2013.
https://doi.org/10.1088/0957-4484/24/24/245701

[25] George, S. M. "Atomic Layer Deposition: An Overview", Chemical Reviews 110(1), pp. 111–131, 2010.
https://doi.org/10.1021/cr900056b

[26] Liu, M., Li, X., Karuturi, S. K., Tok, A. I. Y., Fan, H. J. "Atomic Layer Deposition for Nanofabrication and Interface Engineering", Nanoscale, 4(5), pp. 1522–1528, 2012.
https://doi.org/10.1039/c2nr11875k

[27] Kim, H., Lee, H., Maeng, W. J. "Applications of Atomic Layer Deposition to Nanofabrication and Emerging Nanodevices", Thin Solid Films, 517(8), pp. 2563–2580, 2009.
https://doi.org/10.1016/j.tsf.2008.09.007

[28] Boyadjiev, S. I., Kéri, O., Bárdos, P., Firkala, T., Gáber, F., Nagy, Z. K., Baji, Z., Takács, M.; Szilágyi, I. M. "TiO_2/ZnO and ZnO/TiO_2 Core/Shell Nanofibers Prepared by Electrospinning and Atomic Layer Deposition for Photocatalysis and Gas Sensing", Applied Surface Science, 424(2), pp. 190–197, 2017.
https://doi.org/10.1016/j.apsusc.2017.03.030

[29] Szilágyi, I. M., Nagy, D. "Review on One-Dimensional Nanostructures Prepared by Electrospinning and Atomic Layer Deposition", Journal of Physics-Conference Series, 559, pp. 1–13, 2014.
https://doi.org/10.1088/1742-6596/559/1/012010

[30] Stober, W., Fink, A. "Controlled Growth of Monodisperse Silica Spheres in the Micron Size Range", Journal of Colloid and Interface Science, 26(1), pp. 62–69, 1968.
https://doi.org/10.1016/0021-9797(68)90272-5

[31] Tolnai, G., Agod, A., Kabai-Faix, M., Kovács, A. L., Ramsden, J. J., Hórvölgyi, Z. "Evidence for Secondary Minimum Flocculation of Stöber Silica Nanoparticles at the Air-Water Interface", Journal of Physical Chemistry, 107(40), pp. 11109–11116, 2003.
https://doi.org/10.1021/jp0344949

[32] Chern, C. S. "Emulsion Polymerization Mechanisms and Kinetics", Progress in Polymer Science, 31(5), pp. 443–486, 2006.
https://doi.org/10.1016/j.progpolymsci.2006.02.001

[33] Brunauer, S., Emmett, P. H., Teller, E. "Adsorption of Gases in Multimolecular Layers", Journal of the American Chemical Society, 60(2), pp. 309–319, 1938.
https://doi.org/10.1021/ja01269a023

[34] Puurunen, R. L. "Growth per cycle in atomic layer deposition: A theoretical model", Chemical Vapor Deposition, 9(5), pp. 249–257, 2003.
https://doi.org/10.1002/cvde.200306265

[35] Johnson, R.W., Hultqvist, A., Bent, S.F. "A brief review of atomic layer deposition: From fundamentals to applications", Materials Today, 17(5), pp. 236–246., 2014.
https://doi.org/10.1016/j.mattod.2014.04.026

[36] Shokri, B., Abbasi Firouzjah, M., Hosseini, S. I. "FTIR Analysis of Silicon Dioxide Thin Film Deposited by Metal Organic-Based PECVD", 2015, October. [online] Available at: http://www.ispc-conference.org/ispcproc/papers/791.pdf [Accessed: 16 January 2019]

[37] Yang, L.-L., Lai, Y.-S., Chen, J. S., Tsai, P. H., Chen, C. L., Chang, C. J. "Compositional Tailored Sol-Gel SiO_2–TiO_2 Thin Films: Crystallization, Chemical Bonding Configuration, and Optical Properties", Journal of Materials Research, 20(11), pp. 3141–3149, 2011.
https://doi.org/10.1557/JMR.2005.0393

[38] Khaled, S. M., Sui, R., Charpentier, P. A., Rizkalla, A. S. "Synthesis of TiO_2 - PMMA Nanocomposite: Using Methacrylic Acid as a Coupling Agent", Separation and Purification Technology, 23(7), pp. 3988–3995, 2007.
https://doi.org/10.1021/la062879n

[39] Duan, G., Zhang, C., Li, A., Yang, X., Lu, L., Wang, X. "Preparation and Characterization of Mesoporous Zirconia Made by Using a Poly(Methyl Methacrylate) Template", Nanoscale Research Letters, 3(118), pp. 118–122, 2008.
https://doi.org/10.1007/s11671-008-9123-7

[40] Lv, Y., Xu, P., Ren, G., Chen, F., Nan, H., Liu, R., Wang, D., Tan, X., Liu, X., Zhang, H., Chen, Z. "Low-Temperature Atomic Layer Deposition of Metal Oxide Layers for Perovskite Solar Cells with High Efficiency and Stability under Harsh Environmental Conditions", ACS Applied Materials and Interfaces, 10(28), pp. 23927–23937, 2018.
https://doi.org/10.1021/acsami.8b07346

[41] Zhao, X., Selcuk, S., Selloni, A. "Formation and Stability of Reduced TiO_x Layers on Anatase TiO_2(101): Identification of a Novel Ti_2O_3 Phase", Physical Review-Materials, 2, ID. 015801, 2018.
https://doi.org/10.1103/PhysRevMaterials.2.015801

[42] Justh, N., Firkala, T., László, K., Lábár, J., Szilágyi, I.M. "Photocatalytic C_{60}-amorphous TiO_2 composites prepared by atomic layer deposition", Applied Surface Science, 419, pp. 497–502, 2017.
https://doi.org/10.1016/j.apsusc.2017.04.243